Photoaffinity enabled transcriptome-wide identification of splice modulating small molecule-RNA binding events in native cells

Raven Shah[1], Wanlin Yan[1], Joyce Rigal[1], Steve Mullin[1], Lin Fan[1], Lynn McGregor[1], Andrew Krueger[1], Nicole Renaud[1], Andrea Byrnes[1]*, Jason R. Thomas[1]*

* co-corresponding authors: andrea.byrnes@novartis.com; jason.thomas@novartis.com

Novartis Biomedical Research, Discovery Sciences, Cambridge, MA, USA

Content: Supplementary Figures **S1-9** and chemical probe synthesis/characterization (**Section II**). Excel tables provided with detailed information to reproduce plots in main text:

1. Table of 161 RNA hits enriched above **B1-PAL** & competed by **NV1**
2. Table of 235 RNAs competed by (**NV1** & not **NV2**) & differentially spliced
3. Differentially spliced genes (DSGs) for all **NV1-PAL** treated samples compared to **B1-PAL** (background) treatment (DEXseq [1] output)
4. Differential enrichment (Chem-CLIP) and expression (RNAseq) log2FCs & p-values provided for all sample contrasts
5. TPM values for Chem-CLIP & RNAseq samples (all biological replicates)
6. SHAPE reactivity values for DMSO- & **NV1**-treated samples from ΔSHAPE-MaP experiments

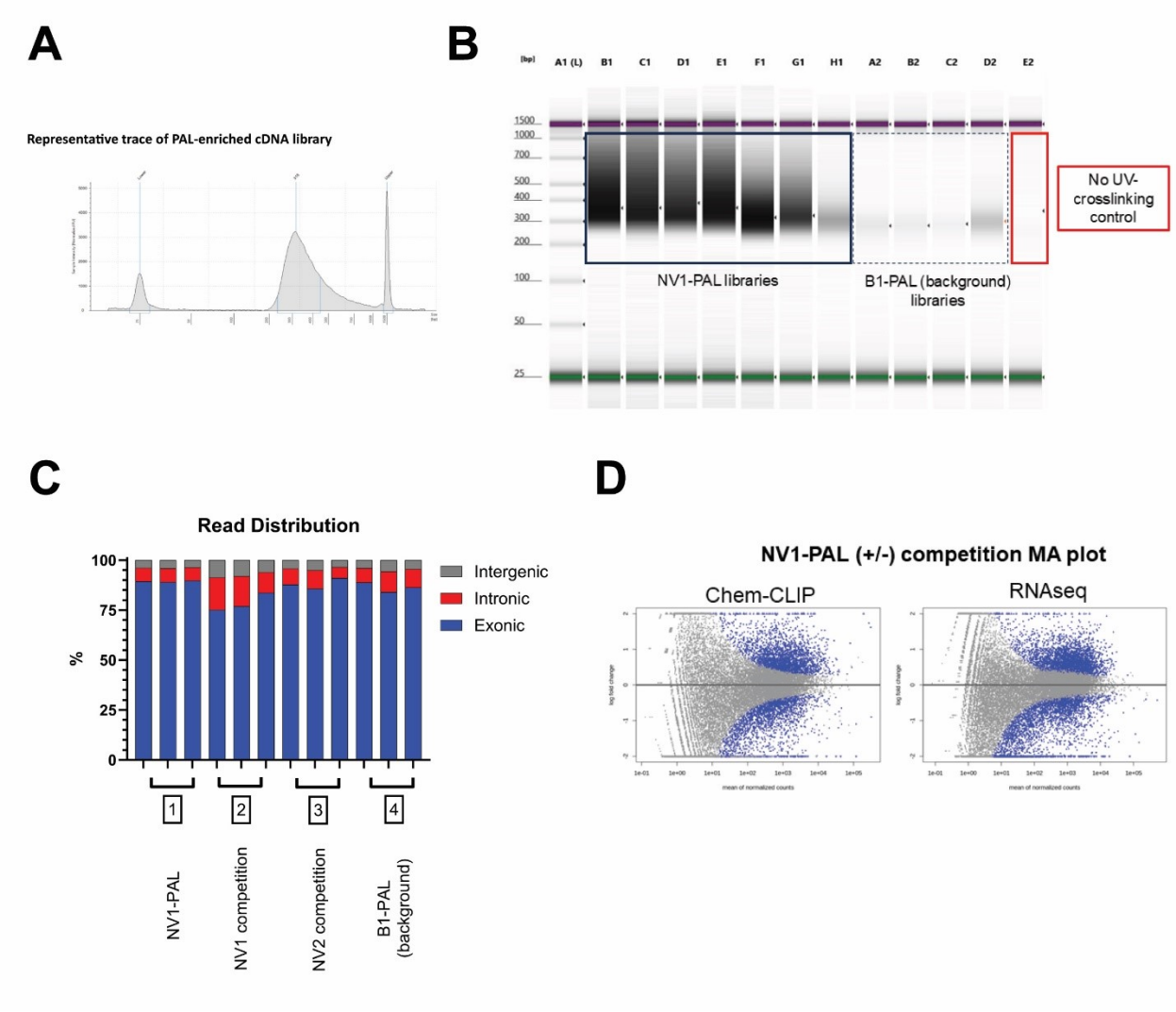

Supplemental Figure 1. Quality control assessment of PAL-based Chem-CLIP libraries. (A) Representative chromatogram from TapeStation trace of final PAL-based Chem-CLIP cDNA library prior to pooling and sequencing (B) PCR amplified product of final PAL-based Chem-CLIP cDNA libraries visualized on TapeStation gel. Average fragment sizes are 300-500 bp per library with final product concentration ranging from 14-150 nM. Increased final product observed for **NV1-PAL** enriched libraries relative to empty PAL control. Little to no product observed in no UV irradiation or DMSO controls (C) Read distribution of PAL-based chem-CLIP libraries analyzed in this study. (D) Minus-Average (MA) plots (normalized counts *vs.* $\log_2$ fold changes) of respective RNA transcripts to evaluate magnitude of fold changes relative to mean changes in enrichment relative to **NV1-PAL** with 20 μM **NV1-PAL** samples. MA plots were visualized to compare differential profiles of parallel processed PAL-based Chem-CLIP *vs.* RNAseq libraries for **NV1-PAL** treated samples without or with 20 μM **NV1-PAL**.

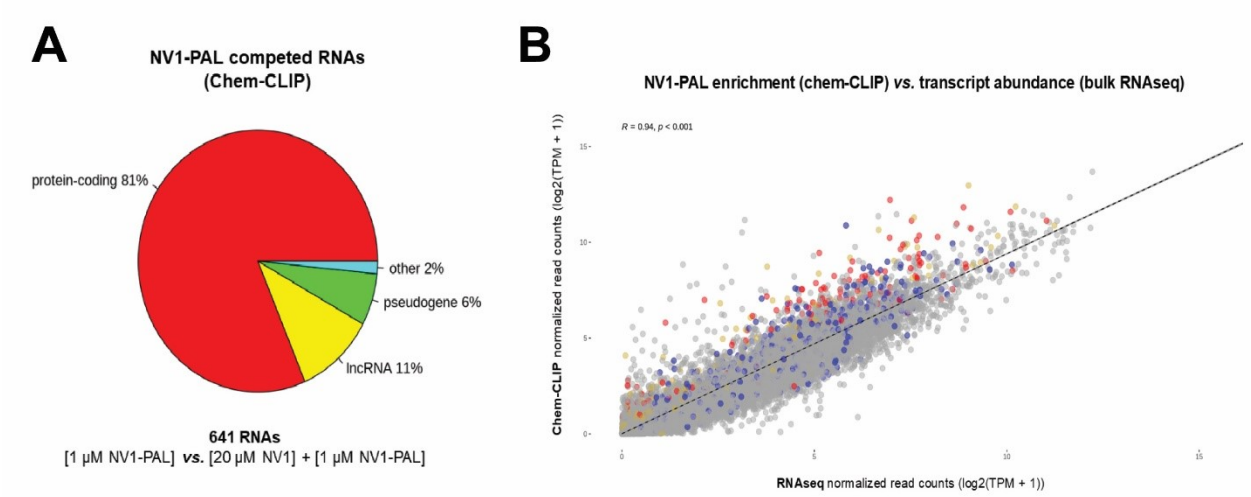

C

Δ transcript expression (DEGs)	Δ expression of NV1 competed RNAs
Up-regulated	1
Down-regulated	212 (35%)
No change	428 (66%)

Supplemental Figure 2. Descriptive RNA hit profiles of NV1-PAL probe. (A) RNA biotype distribution of **NV1** competed RNAs. (B) Scatterplot of **NV1-PAL** normalized read counts from PAL-based chem-CLIP experiments *vs.* the normalized read-counts from the parallel RNAseq experiment. R^2=0.94, suggesting strong association between degree of PAL labeling and total transcript abundance. Grey points = no significance, dark yellow = RNAs enriched by **NV1-PAL** over **B1-PAL**, blue = RNAs competed by **NV1**, red = enriched and competed RNAs. Significance = $\log_2$FC ≥ 1.0 and p-values ≤ 0.05. (C) Distribution of changes in expression for **NV1-PAL** competed RNAs.

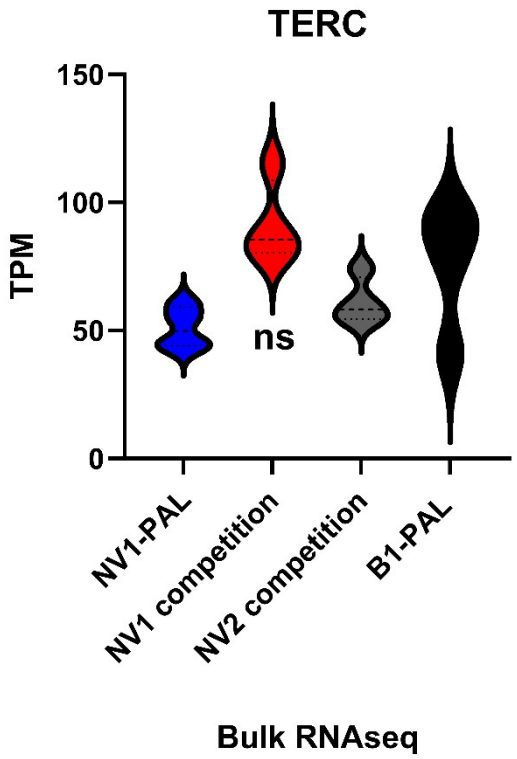

Supplemental Figure 3. TPM values (RNAseq) of TERC lncRNA across PAL treatment conditions. (A) TPM values of total TERC transcripts across compound treatments. 'ns' denotes a non-significant p-value for differences in TPM values (transcriptome-wide student T-test).

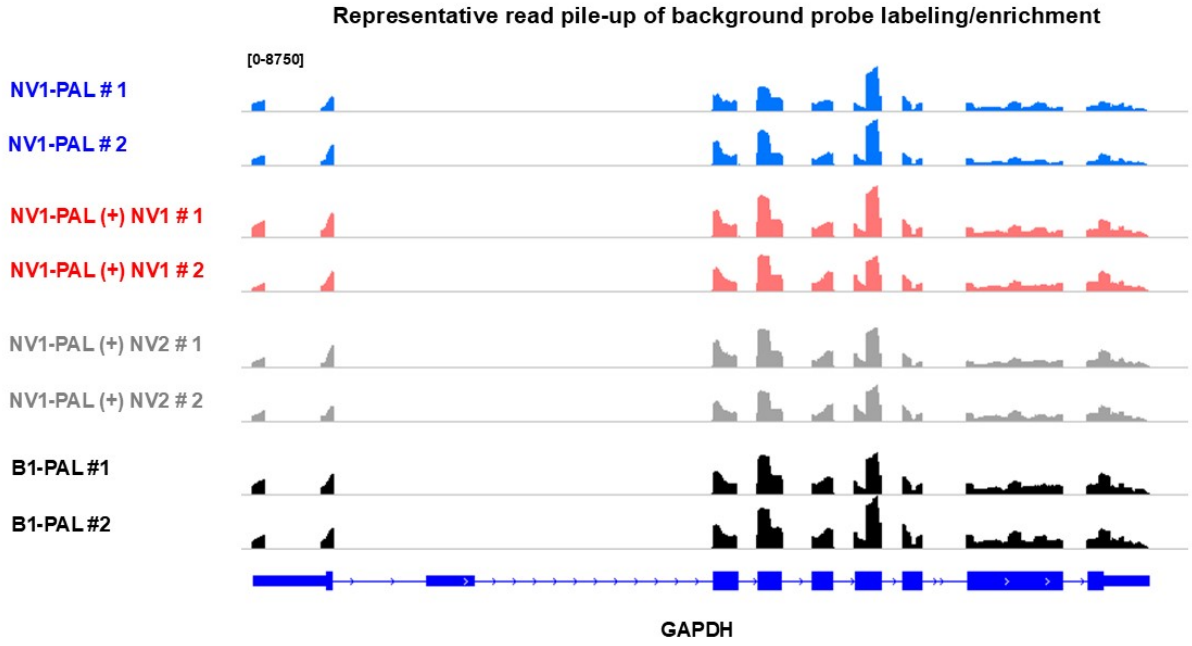

Supplemental Figure 4. Read density of *GAPDH* locus across all treatment conditions. Comparable read counts across all treatment conditions at GAPDH, demonstrating background signal in this assay.

A

DMSO (v/v) or NV1	NAI or DMSO (v/v)	Initial reads	% Pass trim	% Uniquely aligned	% PCR duplicates	Final reads	% Covered bases	Mean coverage
DMSO	DMSO	18,530,655	99.84%	0.38%	42.07%	40,970	100.00%	5,655
DMSO	DMSO	20,218,636	99.87%	0.44%	40.71%	52,508	100.00%	7,173
DMSO	NAI	18,979,226	99.83%	0.34%	43.91%	36,611	100.00%	4,898
DMSO	NAI	22,471,126	99.85%	0.31%	44.01%	38,529	100.00%	5,257
NV1	DMSO	20,212,955	99.84%	0.50%	42.54%	57,504	100.00%	7,635
NV1	DMSO	20,133,344	99.81%	0.42%	44.49%	46,909	100.00%	6,274
NV1	NAI	22,037,658	99.84%	0.33%	45.98%	38,901	100.00%	5,359
NV1	NAI	21,659,504	99.83%	0.28%	43.79%	33,885	100.00%	4,654

B

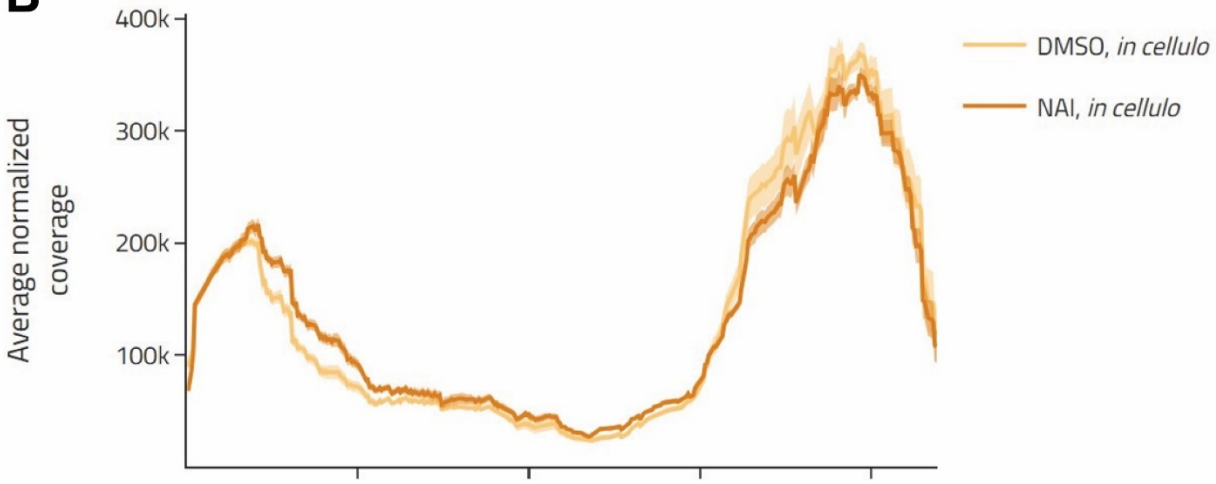

C

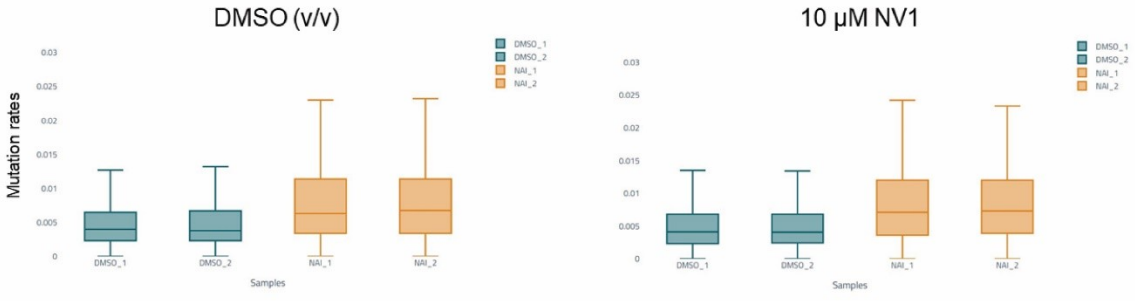

Supplemental Figure 5. Cellular SHAPE-MaP library quality control assessment. (A) Summary statistics of sequencing & read alignment at TERC locus for all SHAPE-MaP samples. (B) Normalized read coverage averaged across biological replicate (N=2 for each (DMSO and 10 μM **NV1** treated sample) +/- NAI) at TERC locus. Read coverage is plotted 5' --> 3' (TERC lncRNA). (C) Mutation frequency for DMSO and **NV1** treated samples, comparing mutation rate of NAI (acylating reagent) treated samples relative to DMSO.

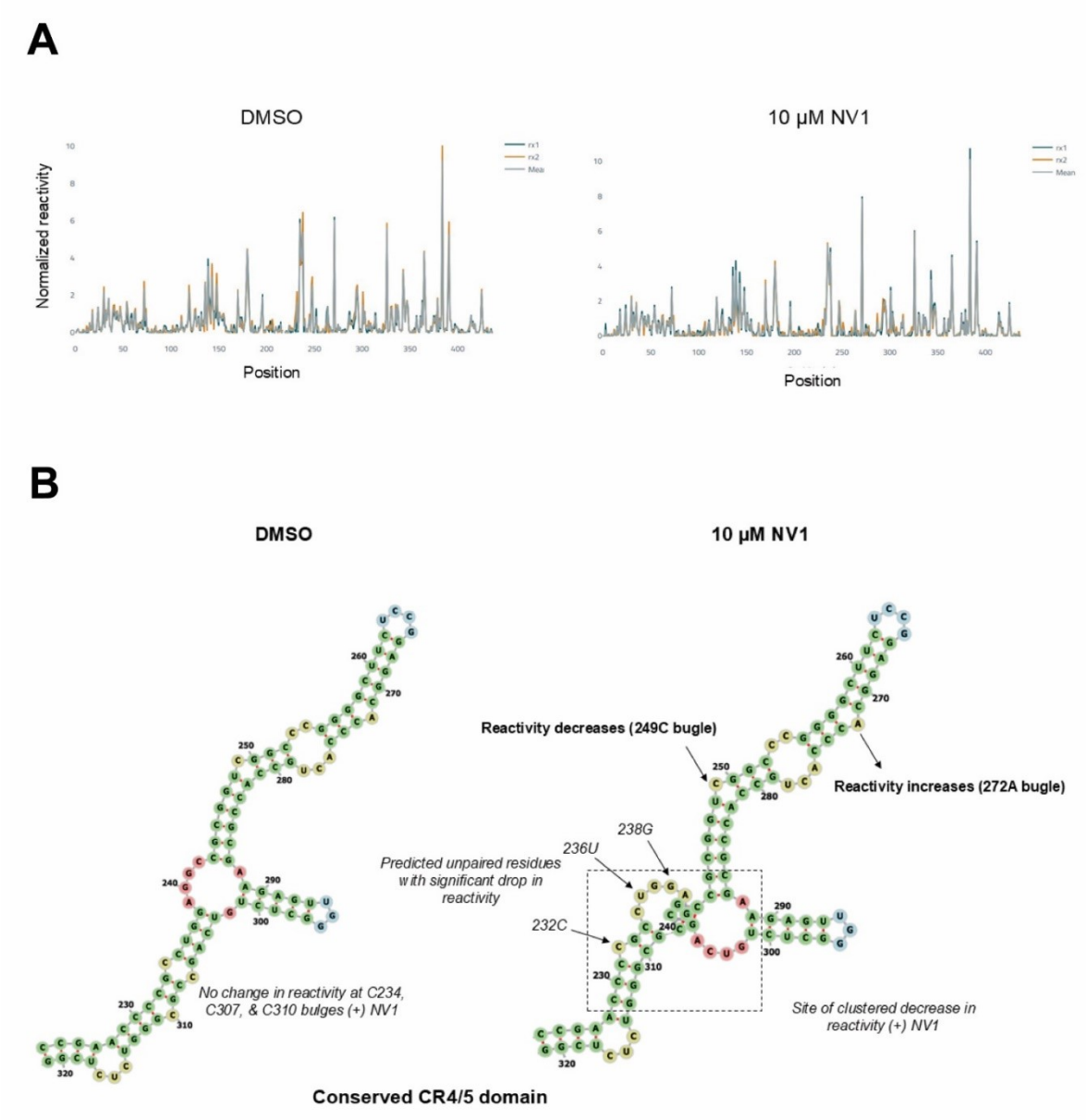
A
DMSO
10 µM NV1
Normalized reactivity
Position
Position
B
DMSO
10 µM NV1
Reactivity decreases (249C bugle)
Reactivity increases (272A bugle)
238G
236U
Predicted unpaired residues with significant drop in reactivity
232C
No change in reactivity at C234, C307, & C310 bulges (+) NV1
Site of clustered decrease in reactivity (+) NV1
Conserved CR4/5 domain

Supplemental Figure 6. Cellular SHAPE-MaP reactivity profiles and secondary structural renderings of TERC CR4/5 domains with SHAPE constraints for DMSO and NV1 treated samples. (A) Normalized reactivity profiles (N=2) for DMSO and 10 μM **NV1** treated samples. For each condition, the reactivity trace of each individual replicate is shown with the mean signal (gray) across the two replicates. (B) SHAPE-MaP constrain secondary structure rendering of CR4/5 domain with DMSO (left) or 10 uM NV1 (right) treatment. Boxed region indicates site of significant clustered changes in NAI reactivity in the presence of NV1. The bulged residues 249C is suspected to be important for compound engagement as this residue has the most significant reduction in reactivity. Secondary structures with SHAPE reactivity constraints were visualized using Forna [2]. Nucleotides are colored based on structure (stems = green, multiloops/junctions = red, interior loops = yellow, hairpin loops = blue, 5' & 3' unpaired region = orange).

a

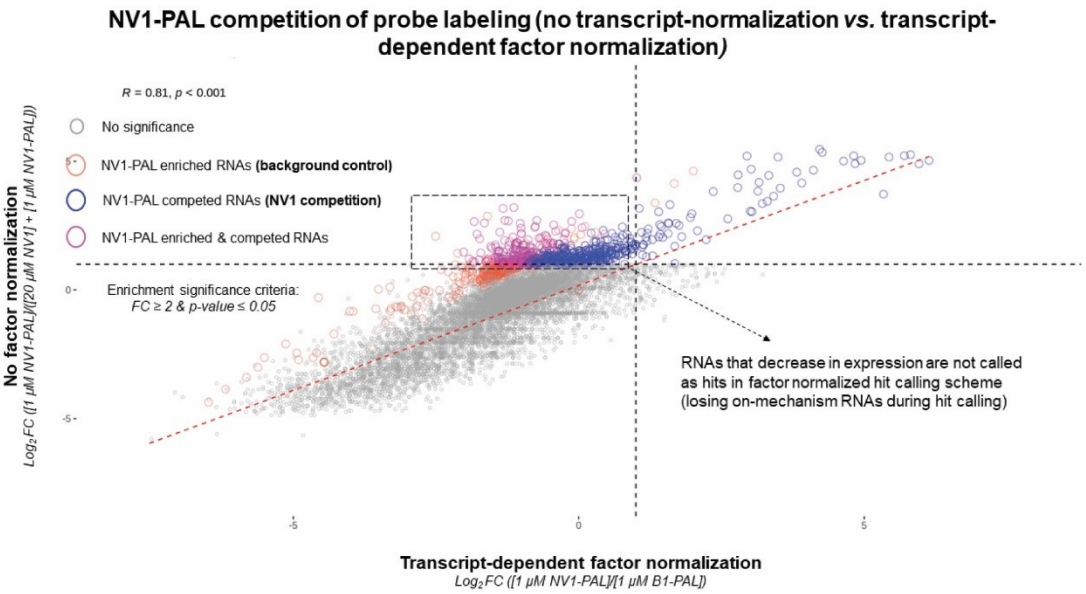

b

Sample code for Implementation of RNA-dependent factor normalization using DESeq2 to normalize read counts of probe-enriched RNAs by covariation in transcript abundance across samples:

1) Create read count table from RNAseq .bedfiles to scale covariation in read counts of targeted enrichment (chem-CLIP) studies

2) Define normalization matrix in DESeq object for factor normalization

3) Set size factors or assign to default & run differential enrichment analysis

```
for (k in 1:dim(normalization_matrix)[2]) {
        normalization_matrix1[,k] <- normalization_matrix[,k] + 1
}       #add one to each read count value per transcript
normalization_matrix2 <- normalization_matrix1 / exp(rowMeans(log(normalization_matrix1)))
        #divide out geometric mean for each transcript
group <- factor(rep(1:3,each=2))
condition <- factor(rep(rep(c("sample","control"),each=3)))
d <- data.frame(group, condition)
as.data.frame(d)
dds <- DESeqDataSetFromMatrix(countData=round(chem-CLIP_matrix),
                colData=d,
                design=~condition,
)
        #define chem-CLIP matrix with raw read counts per transcript
normalizationFactors(dds) <- as.matrix(normalization_matrix2)
        #define normalization matrix in DESeq2 object for scaling differential enrichment
dds <- DESeq(dds)
        #construct object with normalized read count values that can be used as input for differential enrichment analysis
```

c

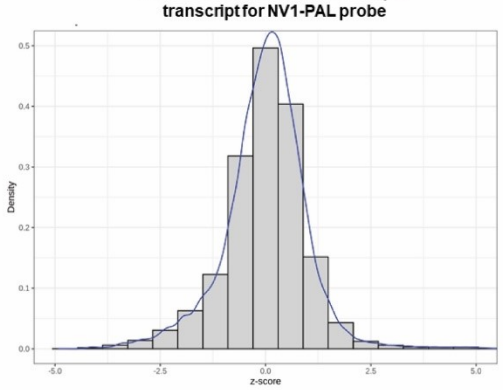

Z-score calculation:

1) Enrichment ratio$_{transcript}$ = Log2(chem-CLIP (TPM+1) $_{transcript}$ / RNAseq (TPM+1) $_{transcript}$)

2) Filter for probe-enrichment (TPM) > 0

3) Calculate z-score based on filtered RNAs (~17k RNAs) and assign cut-off for hit calling strategy

Supplemental Figure 7. Alternative hit calling strategies explored using transcript-dependent factor normalization & z-score analysis. (A) Scatterplot of $\log_2$ fold-change of 1 μM **NV1-PAL** without or with 20 μM **NV1** without (y-axis) or with (x-axis) factor normalization**.** In this strategy, RNAs with a higher abundance relative to the control sample are not called as hits regardless of degree of probe enrichment/labeling competition. (B) Example of R code to factor scale probe enrichment/degree of competition of probe labeling using parallel RNAseq analysis. Raw read counts from the bulk RNAseq are transformed and defined as the normalization matrix in the DESeq2 object prior to running the differential enrichment analysis. (C) An enrichment ratio is calculated ($\log_2$ (chem-CLIP$_{TPM+1}$ /RNAseq$_{TPM+1}$)) with the assumption that specific or high-affinity compound RNA targets will have an increased TPM relative to bulk RNAseq. Z-score thresholds can be set and compared to DESeq2 output. These strategies did not improve hit calling efficiency.

A

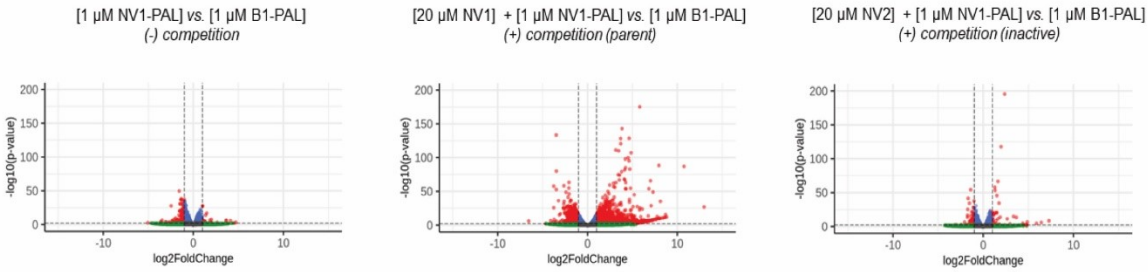

Expression change	NV1-PAL (-) competition	NV1-PAL (+) competition (parent)	NV1-PAL (+) competition (inactive)
UP	108	2197	105
DOWN	338	1387	156

9161 total differentially spliced genes in NV-8 PAL treated samples (+/- competition)

B

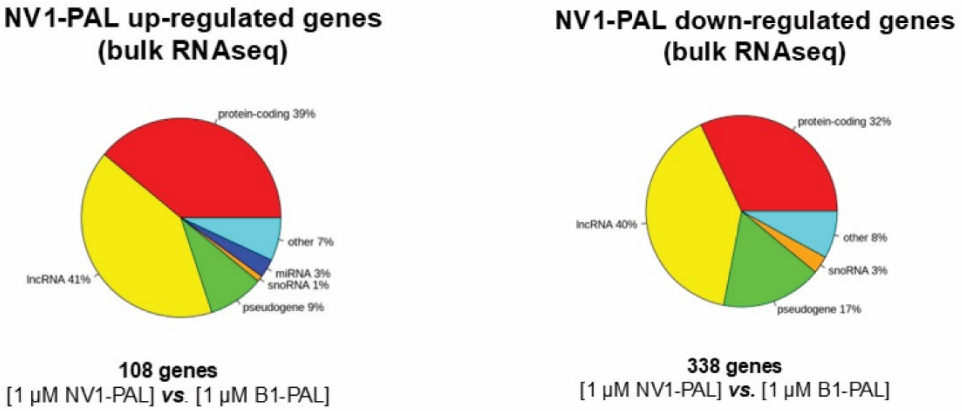

108 genes
[1 µM NV1-PAL] ***vs***. [1 µM B1-PAL]

338 genes
[1 µM NV1-PAL] ***vs.*** [1 µM B1-PAL]

Supplemental Figure 8. Bulk RNAseq expression profiling of parallel processed NV1-PAL treated samples. (A) Volcano plots of **NV1-PAL** treated samples (left), **NV1-PAL** with 20 µM **NV1** samples (middle), **NV1-PAL** with 20 µM **NV2** samples (right) *vs.* B1-PAL. (B) Distribution of biotypes of up-regulated & down-regulated RNAs following **NV1-PAL** relative to **B1-PAL** treatments.

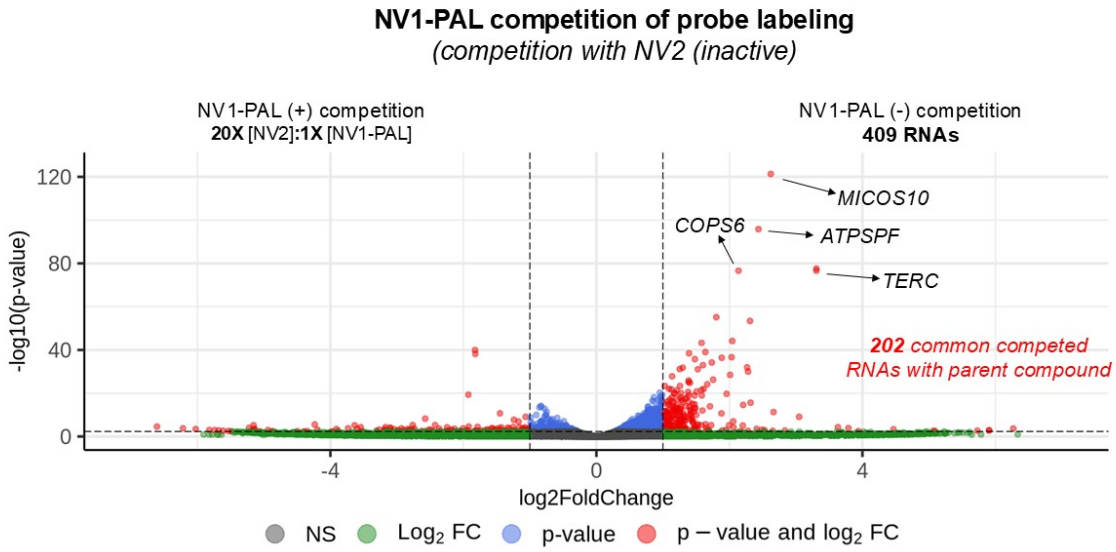

Supplemental Figure 9. Volcano plot of 1 µM NV1-PAL without or with 20 µM NV2. Volcano plot of log_2FC of **NV1-PAL** with 0 µM **NV2** (right quadrant) *vs.* **NV1-PAL** with 20 µM **NV2** (left quadrant). The RNAs in the right quadrant represent higher labeling in the **NV1-PAL** with 0 µM **NV2** samples, indicating loss of probe labeling in the presence of **NV2**. The strongest RNAs competed by **NV1** and enriched over **B1-PAL** were also present (COPS6, MICOS10, TERC) in the **NV2** comparison.

Section 2: Synthesis & characterization of chemical photo-probes

Compound NV1-PAL (branaplam series-based photo-probe):

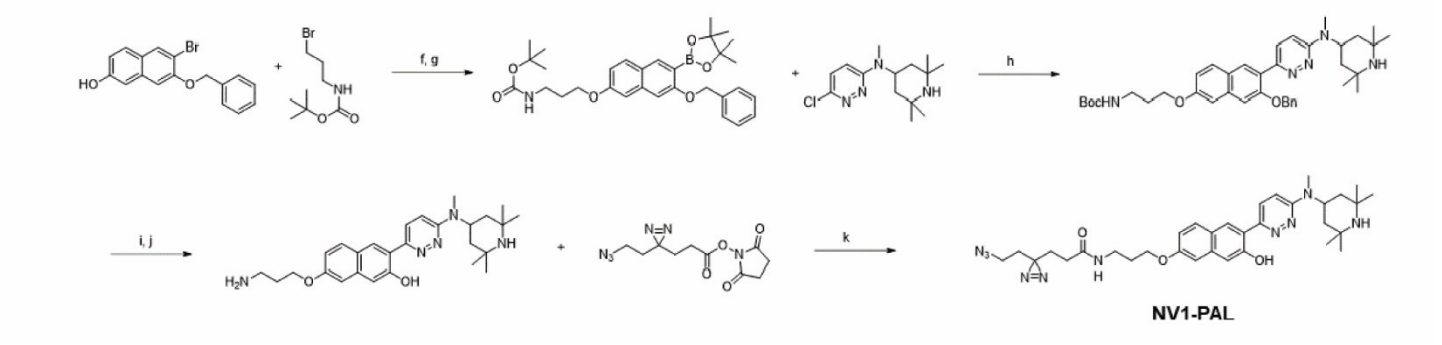

NV1-PAL: 7-(3-aminopropoxy)-3-(6-(methyl(2,2,6,6-tetramethylpiperidin-4-yl)amino)pyridazin-3-yl)naphthalen-2-ol (30 mg, 0.056 mmol) and 2,5-dioxopyrrolidin-1-yl 3-(3-(2-azidoethyl)-3H-diazirin-3-yl)propanoate (14.1 mg, 0.05 mmol) were dissolved in DMF (2mL), DIPEA (29 uL, 0.168 mmol) was added to the solution. The mixture was stirred for 1.5 hours at room temperature. LCMS indicated completion of the reaction. The mixture was diluted in MeOH and purified by RP-HPLC using ammonia hydroxide as modifier. desired peak tailed a lot under basic HPLC, since it was clean reaction, desired peaks were not overlapped with impurity. All fractions with desired mass were collected, concentrated to afford 22 mg product as a pale yellow solid. ^{1}H NMR (400 MHz, DMSO) δ 13.39 (s, 1H), 8.42 (s, 1H), 8.34 (d, *J* = 9.9 Hz, 1H), 7.98 (t, *J* = 5.6 Hz, 1H), 7.78 (d, *J* = 9.1 Hz, 1H), 7.42 (d, *J* = 9.8 Hz, 1H), 7.18 (s, 1H), 7.10 (d, *J* = 2.4 Hz, 1H), 6.96 (dd, *J* = 8.8, 2.4 Hz, 1H), 5.04 (s, 1H), 4.11 (t, *J* = 6.3 Hz, 2H), 3.23 (q, *J* = 6.8 Hz, 4H), 2.98 (s, 3H), 2.19 (t, *J* = 7.4 Hz, 1H), 1.92 (t, *J* = 7.5 Hz, 4H), 1.72 – 1.60 (m, 6H), 1.24 (m, 16H). LC/MS: retention time: 1.63 min, $[M+1]^+$=629.4, 98% purity; HRMS (m/z): $[M+1]^+$ calcd. for, 629.3676; found, 629.3718;

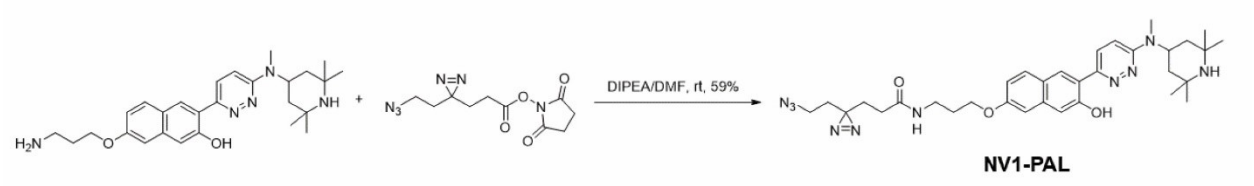

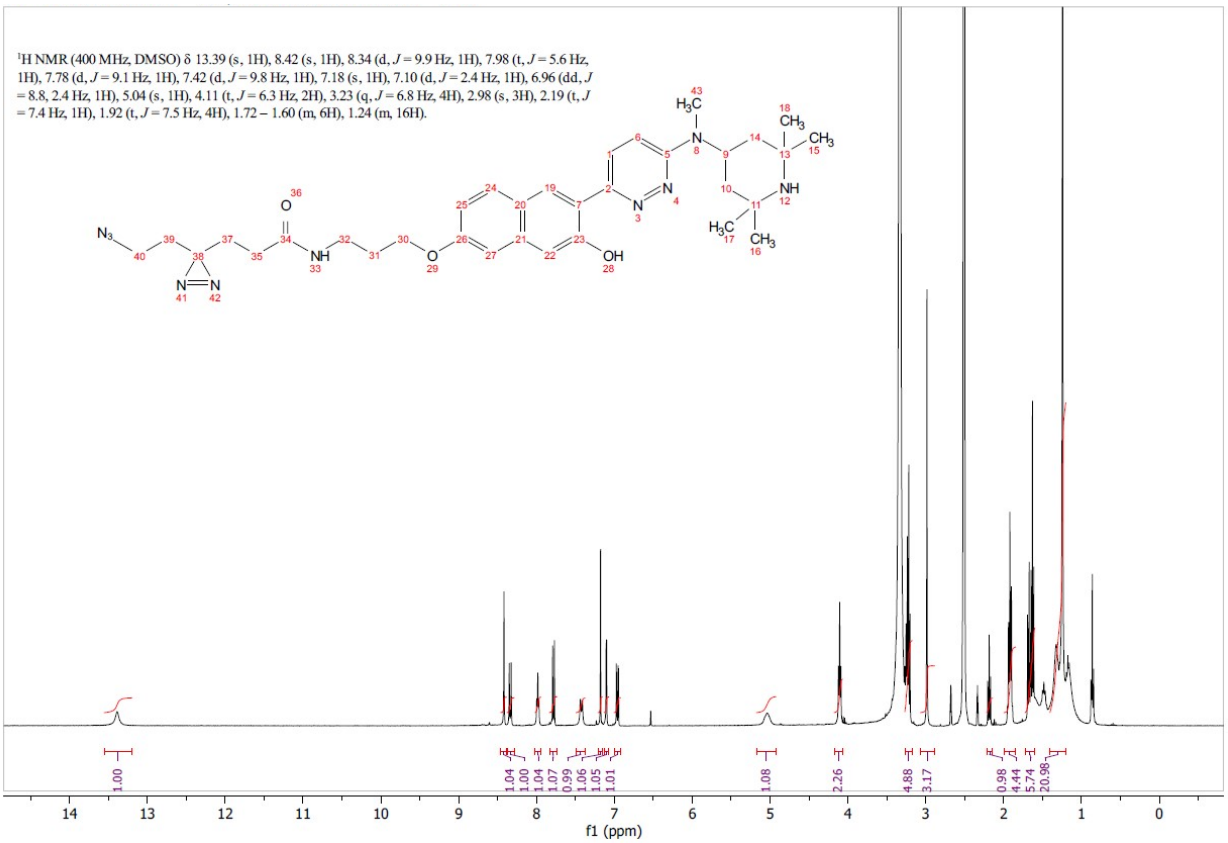
^{1}H NMR (400 MHz, DMSO) δ 13.39 (s, 1H), 8.42 (s, 1H), 8.34 (d, J = 9.9 Hz, 1H), 7.98 (t, J = 5.6 Hz, 1H), 7.78 (d, J = 9.1 Hz, 1H), 7.42 (d, J = 9.8 Hz, 1H), 7.18 (s, 1H), 7.10 (d, J = 2.4 Hz, 1H), 6.96 (dd, J = 8.8, 2.4 Hz, 1H), 5.04 (s, 1H), 4.11 (t, J = 6.3 Hz, 2H), 3.23 (q, J = 6.8 Hz, 4H), 2.98 (s, 3H), 2.19 (t, J = 7.4 Hz, 1H), 1.92 (t, J = 7.5 Hz, 4H), 1.72 – 1.60 (m, 6H), 1.24 (m, 16H).
f1 (ppm)

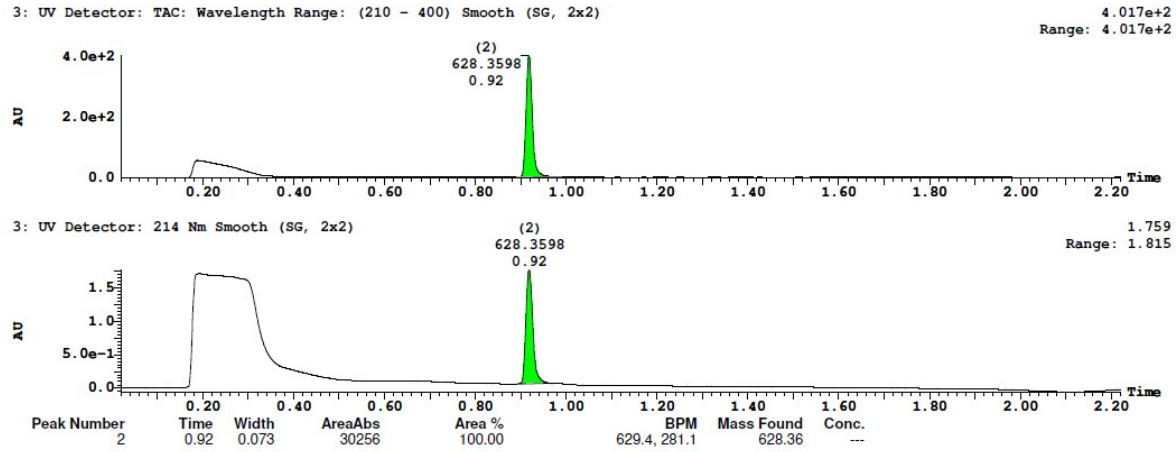
3: UV Detector: TAC: Wavelength Range: (210 - 400) Smooth (SG, 2x2)
4.017e+2
Range: 4.017e+2
(2)
628.3598
0.92
AU
Time
3: UV Detector: 214 Nm Smooth (SG, 2x2)
1.759
Range: 1.815
(2)
628.3598
0.92
AU
Time
Peak Number Time Width AreaAbs Area % BPM Mass Found Conc.
2 0.92 0.073 30256 100.00 629.4, 281.1 628.36 ---

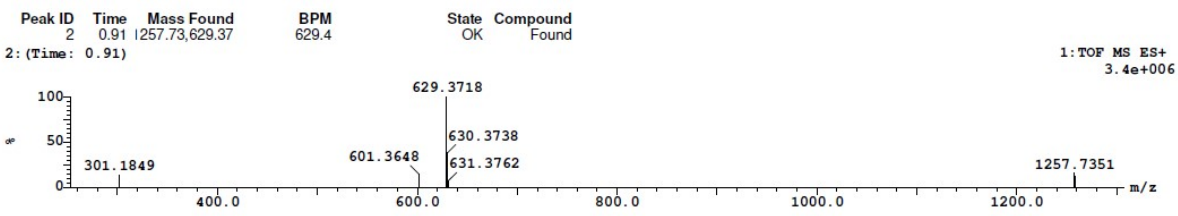
Peak ID Time Mass Found BPM State Compound
2 0.91 257.73,629.37 629.4 OK Found
2: (Time: 0.91)
1: TOF MS ES+
3.4e+006
629.3718
630.3738
631.3762
601.3648
301.1849
1257.7351
m/z

References

1. Anders, S., A. Reyes, and W. Huber (2012). Detecting differential usage of exons from RNA-seq data. Genome Res *22*, 2008-17.
2. Kerpedjiev, P., S. Hammer, and I.L. Hofacker (2015). Forna (force-directed RNA): Simple and effective online RNA secondary structure diagrams. Bioinformatics *31*, 3377-9.